A Non-Nuclear, Solar Powered Mission to Uranus Utilizing the PowerSail - a Large Solar Sail with embedded Solar Cells

John A. Carr[1], Les Johnson[2], Herbert Thomas[3], Mike Baysinger[4], and Thomas Brooks[5]
National Aeronautics and Space Administration, MSFC, AL, 35898, U.S.A

Leo Fabisinski[6], Benjamin Diedrich[7], Peter Capizzo[8], and Jay Garcia[9]
Jacobs, Huntsville AL, 35806, U.S.A.

Michael Benfield[10]
University of Alabama Huntsville, Huntsville AL, 35899, U.S.A.

Powering missions to the outer solar system is a significant challenge. These missions are typically powered by a Radioisotope Thermoelectric Generator (RTG). Though these sources provide stable power regardless of location in space, they are expensive to produce, difficult to integrate, and have both safety concerns as well as negative sociopolitical connotations. Perhaps most importantly, the availability of their fuel, plutonium-238, is scarce. Solar power is often considered a more attractive option. However, photovoltaic generation falls off at the distance from the sun squared. This drives the size of traditional solar generators to infeasible levels for deep space and their utilization at locations deeper the Jupiter is currently non-existent. Herein, a hypothetical solution, the PowerSail, and its application to a non-nuclear Uranus mission is presented. The PowerSail is a marriage of solar sails and thin-film solar cell assemblies. Herein the application of PowerSail spacecraft to a high priority science mission, the Applied Physics Laboratory's Uranus Probe and Explorer, is studied. The overall mission design along with key subsystems design changes are discussed, ultimately showing that a PowerSail could be utilized as a non-nuclear option to reach destinations very deep in our solar system. Key needed technology developments to make the PowerSail and such a mission a reality are given.

I. Introduction

Planetary science missions currently being targeted are grouped into four categories: (1) outer planets, (2) inner planets, (3) Mars, and (4) small bodies [1, 2]. Of the small bodies, Jupiter Trojans and dwarf planets are of interest to the science community. Within the outer plants, ice giants like Uranus, and ocean worlds, such as Enceladus, are of particular interest. Many of these destinations remain largely underexplored. For example, both Uranus and Neptune have been explored only by one fly-by space probe, Voyager 2 (~1986-1989) with ~1970's era technology [3-6]. In fact, within the 2023-2032 decadal strategy for planetary science and astrobiology, the committee "prioritizes the

[1] Center Deputy Chief Technologist, MSFC Science and Technology, Corresponding Author: john.a.carr@nasa.gov.
[2] Center Chief Technologist, MSFC Science and Technology
[3] AST Aerospace Flight Systems, MSFC Advanced Concepts Office
[4] AST Aerospace Flight Systems, MSFC Advanced Concepts Office
[5] AST Aerospace Flight Systems, MSFC Advanced Concepts Office
[6] Senior Software Engineer, MSFC Advanced Concepts Office
[7] Staff Engineer, MSFC Engineering Vehicles
[8] Electrical Engineer, MSFC Advanced Concepts Office
[9] Stress Analyst Engineer, MSFC Advanced Concepts Office
[10] Senior Research Engineer, MSFC Advanced Concepts Office

Uranus Orbiter and Probe (UOP) as the highest priority new Flagship mission for initiation in the decade" [2]. This mission has been priority for the last two decades as there is very significant science value to gain [2-8].

Missions to Jupiter and beyond require travel deep into space, reaching distances >5AU. To power deep space missions, spacecraft traditionally employ Radioisotope Thermoelectric Generators (RTGs), such as the SNAP-19 used on the Pioneer missions, the MHW-RTG used on Voyager, or the GPHS-RTG used on Ulysses, Galileo, Cassini-Huygens, and New Horizons [9-11]. Though these sources safely provide stable power indiscriminate of location, they are expensive to produce and integrate [12] and have significant impact to mission schedule [13]. More importantly, the widely used RTG fuel is non-weapons grade plutonium-238 (Pu-238), which is a scarce material that must be specifically produced; it is not naturally occurring nor harvestable from nuclear waste [13, 14]. In the early phases of deep space exploration, the United States was producing as much as 20kg of Pu-238 per year, with plans to more than double production. However, the U.S. ceased production in ~1988 and subsequently began purchasing a small amount of Pu-238 from Russia [15, 16]. Russia stopped its own production in 1993 and the U.S.'s interim purchases stopped. As of 2019, the U.S. had only ~35kg left in stockpile and, even as of 2014, only part of this stockpile still meet NASA requirements for use [15]. This is enough for just ~600W of mission power and most is already allocated for planned missions. Efforts to restart U.S. Pu-238 production were picked up circa 2012. As of 2019, the total reported capability was just 400g per year [17]. Efforts to scale to 1.5kg per year by 2025 are ongoing [17, 18]. However, for reference, NASA's current multi-mission-RTG design utilizes 3.5 to 4.8kg of Pu-238 for 110W of electrical power [12, 15]. At our current rates, it will take over 25 years to produce enough nuclear material for just one 330W deep space mission, let alone missions double that size which simply aren't feasible with current production rates.

Solar power is a more attractive power generation option, unfortunately generation falls off rapidly at $1/\text{distance}^2$ from the sun [19], thus driving a huge increase in the required size of solar arrays. The Juno spacecraft brought solar panels to Jupiter, where solar intensity is just ~3.7% that of Earth [19, 20]. This is the deepest a solar powered spacecraft has travelled. Europa Clipper, which has just launched in 2024, is also traveling via solar power to Jupiter [21] [22]. However, moving deeper is an exponential challenge. At Saturn only 1.1% irradiance remains, and at Pluto, just 0.06% [19]. This quickly drives the size of traditional solar generators to infeasible levels and has left their utilization at these deep locations non-existent. Hence our reliance on scarce nuclear fuel. But what if we can change the possible?

II. A Solution: the PowerSail

A disruptive solution is the PowerSail (**Fig. 1**). The PowerSail is the marriage of two technology development efforts: solar sails [23-29] and thin-film photovoltaic assemblies [30-38]. Solar sails, which form the basis of the architecture, have been developed for programs like NanoSail-D [23], LightSail [29], and NEAScout [26] and are currently being scaled for programs such as the Solar Cruiser mission [28]. When coupled with thin, flexible solar cells, such as those being developed for the Lightweight Integrated Solar Array and anTenna (LISA-T) project [39-42], a large-scale sail with embedded solar power generators is formed: a *PowerSail*. The PowerSail can be larger than 10 tennis courts and is thinner than a sheet of paper. With embedded power routing, supporting electronics, targeted GN&C, and a sailcraft bus, the PowerSail architecture is completed. The PowerSail can provide a science enabling amount of power in deep space, *without the use of nuclear fuel*. What's more, extremely large PowerSails could be potentially utilized for non-nuclear, fast transit for crewed missions to Mars [43-45]. Herein, the PowerSail architecture and its associated PowerSail-Craft for a non-nuclear mission to Uranus is described.

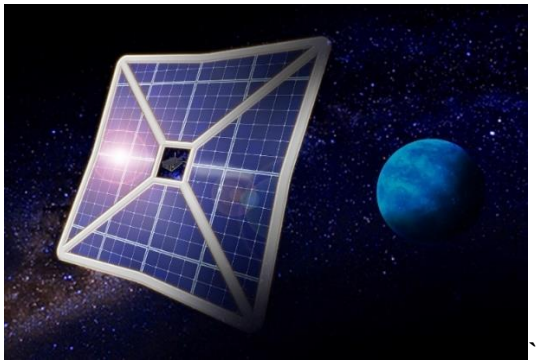

Fig. 1: Rendering of PowerSail Spacecraft

The PowerSail is comprised of a foldable, rollable <2µm thick colorless polyimide-1 film substrate (**Fig. 2**, left), which is deployed from the spacecraft via rollable composite booms [27, 46, 47]. Photovoltaic cells <100µm thick (Fig. 2, middle) such as Inverted Metamorphic Multijunction (IMM) [34], Copper Indium Gallium Di-selenide (CIGS) [31], or silicon DragonSCALES [33] are embedded onto the entire area of the polyimide substrate (Fig. 2, right). A protective coating <20µm thick is applied atop the cells [42], and copper power routing traces are embedded on the backside of the substrate. Laminated, looped silver ribbon is used to create welded connections between each cell. Eventually, a fully additive or printed manufacturing process is envisioned to create these very large, thin-film solar array [48, 49]. Such a process could also incorporate additively manufactured solar cells such as Perovskite based formulations [38, 50, 51] and will be essential to scaling very large PowerSail arrays such as those imagined for fast crewed transit to Mars [43, 44] or adapting for in-space manufacturing [49, 50, 52, 53].

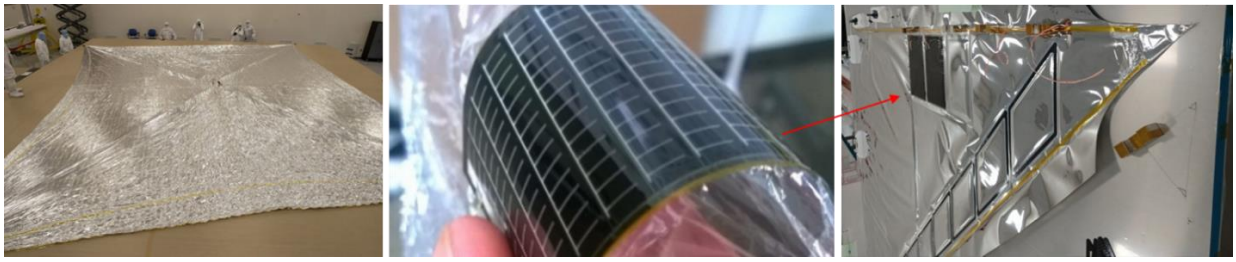

Fig. 2: Substrate and thin-film solar cell assembly that comprise the PowerSail. The NEAScout solar sail deployed (Left). A 'LISA-T' Thin-film solar cell stack up (Middle). A 'LISA-T' stack up embedded on a solar sail (Right).

Fig. 3 shows modelled estimates of power generation versus solar distance (in AU) of a 'NEAScout class' (blue triangles, 86m^2 total area) and 'Solar Cruiser clas's (blue squares, 1400m^2 total area) PowerSail compared to that of RTG based planetary missions and both the SOA Juno solar array as well as projected levels for emerging flexible rollout solar arrays. A NEAScout class PowerSail is competitive in power generation, without dependence on plutonium, out to ~10AU (Saturn) and potentially as far as ~19AU (Uranus) – **enabling solar power at Saturn and deeper**. At first look, the Fold Out Solar Array appears to outperform the NEAScout class PowerSail as it is higher power, but mass is *significantly* different between the two and severely limits SOA (**Fig. 4).** Scaling to the Cruiser class PowerSail (1400m^2 total area) extends capability to ~30AU (Neptune) and could reach as far as ~40AU (Pluto). The Jet Propulsion Laboratory [1] has defined a need for >20kW (at 1AU) solar arrays for small body missions and >50kW (at 1AU) for outer planets. The former is directly achievable with a NEAScout class PowerSail and the latter with a Cruiser PowerSail. This translates to ~200 to >500W of mission power at bodies of interest.

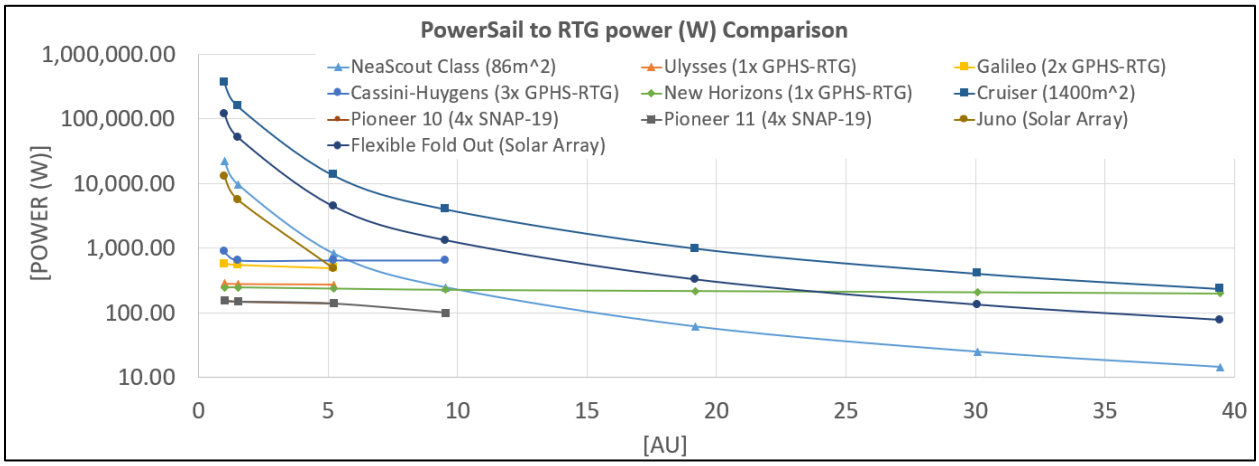

Fig. 3: PowerSail and SOA deep space power generation options power vs. AU.

As seen in **Fig. 3** solar array technologies currently in development, such as the MegaROSA or MegaFlex semi-flexible roll-out or fold-out arrays [54-57], can conceptually supply as much as 150kW at 1AU. However, the proposed PowerSail architecture can supply this power with a *mass savings of greater than 300%*. At these high-power

generation levels, JPL has defined a need of just that, for >3x lower mass solar arrays for deep space missions – especially for those utilizing SEP [58]. In short, non-nuclear, solar powered missions to deep space cannot currently close due to mass limitations. The lightest SOA arrays to date have a specific power of just ~100W/kg. The emerging rollout arrays currently in development are projected to reach ~150W/kg, making their utilization for these deep missions infeasible. The NEAScout class PowerSail is projected at >400W/kg, more than meeting the 3x target and making it mass competitive with nuclear RTGs out to about 19AU (Uranus). The Cruiser class PowerSail could be mass competitive with RTGs out to ~30 (Neptune) or even ~40AU (Pluto).

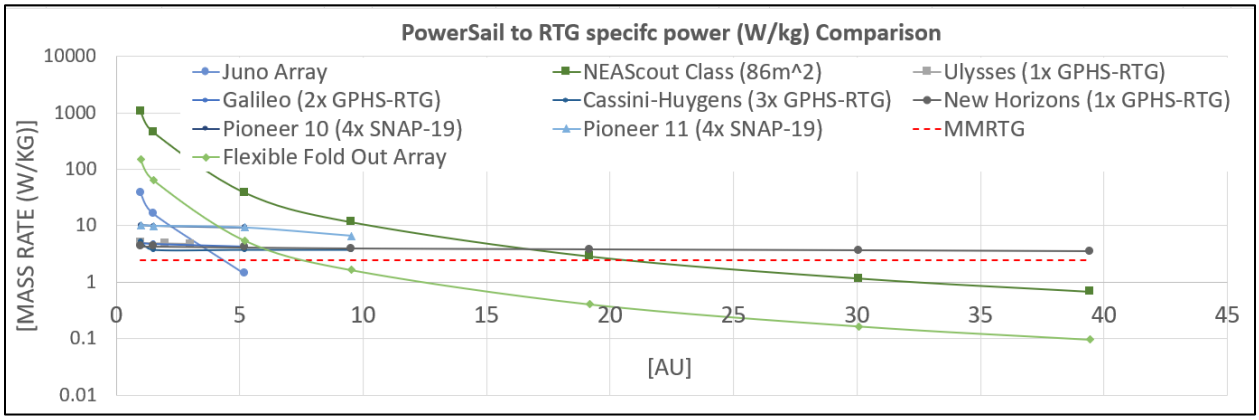

Fig. 4: PowerSail and SOA deep space power generation options specific power vs. AU.

III. A PowerSail Spacecraft to Uranus

As an initial study to determine the usefulness of a PowerSail spacecraft for deep space science, NASA's Marshall Space Flight Center (MSFC) undertook a six-week rapid mission design attempting to utilize a PowerSail spacecraft to bring both an orbital science payload as well as a surface probe to Uranus – without the use of nuclear power. The objective of the study was to determine if such a large gossamer structure could be utilized within similar or better mass and volume constraints as the nuclear option, could close thermal design for very deep, cold exploration without the nuclear source, and to determine if a PowerSail spacecraft could be captured into orbit or would be limited to fly-by mission due to the controllability of such a large gossamer structure. The Uranus PowerSail mission studied followed that outlined in the Uranus Orbiter and Probe decadal survey work [59] by the Applied Physics Laboratory (APL), but swaps the nuclear power source for a PowerSail sized between the NEAScout and Cruise class sails, ~765m^2. For reference, **Table 1** shows the assumed science payload MEL of the Uranus mission.

Table 1: Science subsystem MEL

Mass Estimation List (MEL)			Qty	Unit Mass (kg)	Basic Mass (kg)	MGA (%)	MGA (kg)	Predicted Mass (kg)
7.0 Science Instruments					60.50	10.0%	6.05	66.55
	7.1	Total Instrument Package	1	60.50	60.50	10.0%	6.05	66.55

A. Mission Design

The mission starts with a Falcon Heavy launch, which delivers the PowerSail spacecraft to a maximum C3 of 29.36km^2/s^2. The maximum payload delivered to this C3, and the mass limit for the PowerSail spacecraft, is 8340kg. After C3 delivery, approximately 373 days later, a deep space maneuver is performed to target an unpowered Earth swing-by. Another unpowered gravity assist is then performed at Jupiter, which gives the spacecraft enough energy to reach Uranus in ~11 years. The total interplanetary trip takes 13.5 years, followed by another 5 years in Uranus orbit, bringing the total mission duration to 18.5 years. The overall trajectory and general events are shown in **Fig. 5**.

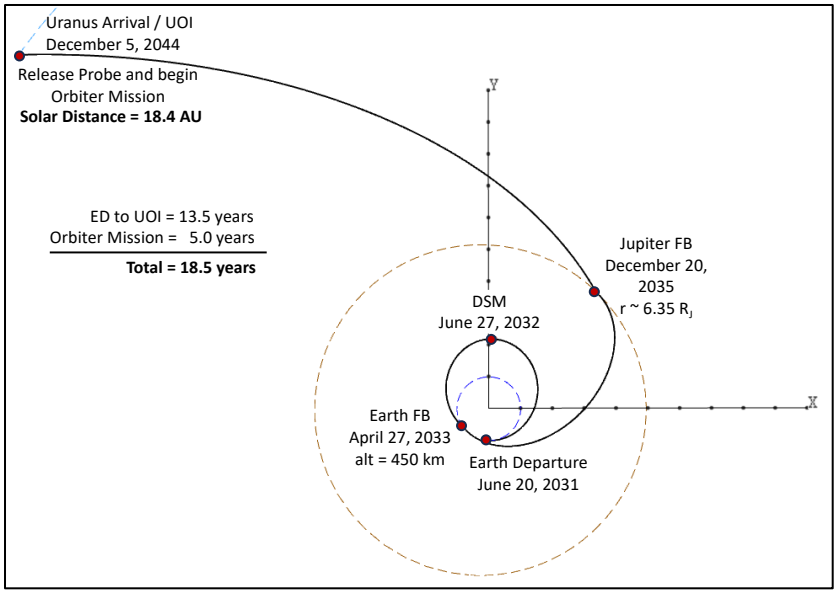

Fig. 5: Nominal Mission Trajectory

Table 2 shows the assumed propulsive events for this mission. The ΔVs are the same as those listed in Exhibit 3-43 of [59]. The propellant required to perform the mission is 4893kg, assuming the maximum start mass of 8340kg. Whereas APLs nuclear power mission study assumed a dual mode Hydrazine monopropellant and Hydrazine/NTO bipropellant propulsion system, this MSFC study utilizes a MMH/NTO bipropellant-only system. This allows the use of the higher thrust R-42 engines (2024, L3Harris Technologies, Inc.) and reduces the thermal propellant management requirements. The higher specific impulse of the RCS engines (R-6F) also reduces the propellant requirements, compared to the monopropellant option. Ansys STK software was used to determine the ground station contact times to NASA's Deep Space Network (DSN) as well as eclipse durations for the entire mission. Angular rates required to view Uranus while in orbit were also computed.

Table 2: Propulsive Mission Events

Event	Mass (kg)	DV (m/s)	Propulsion System	Isp (s)	Propellant (kg)	Engines (#)	Thrust Accel (g)	Burn Time (s)
Launch Cleanup	8340.00	20	RCS	305	55.58	4	0.0011	1889
DSM	8284.42	660	MPS	305	1640.4	2	0.0219	2756.
DSM Cleanup	6644.02	30	RCS	305	66.31	4	0.0014	2254
Earth FB Targeting/Bias	6577.71	50	RCS	305	109.04	4	0.0014	3706
Jupiter FB	6468.67	30	RCS	305	64.56	4	0.0014	2194
UOI Targeting	6404.11	10	RCS	305	21.38	4	0.0014	727
UOI	6382.73	1087	MPS	305	1944.86	2	0.0284	3268
UOI Cleanup	4437.88	45	RCS	305	66.27	4	0.0020	2252
Probe Targeting	4371.61	15	RCS	305	21.87	4	0.0021	743
Probe Separation	4016.74							
Orbiter Divert	4016.74	34	RCS	305	45.4	4	0.0022	1543
PRM	3971.34	171	MPS	305	220.68	1	0.0229	742
PRM Cleanup	3750.66	20	RCS	305	25	4	0.0024	850
Tour	3725.67	47	RCS	305	58.09	2	0.0012	3949
Disposal	3667.58	216	MPS	305	255.52	1	0.0248	859

Unallocated Margin	3412.06	148	MPS	305	164.72	1		554
ACS	3247.34	125	ACS	305	132.91	2	0.0014	9035
				Total Usable Propellant:	4892.58			

It was determined that, with the C3 delivery, propellant budget, and trajectory above, the PowerSail spacecraft could indeed reach Uranus in a timely fashion and could be captured into orbit, enabling a 5 year science mission including both orbital data collection as well as probe delivery.

B. Design and Configuration

The Uranus PowerSail spacecraft design and configuration is based heavily on the RTG spacecraft [59]. It was intentional to keep as much of the 'baseline RTG design', per [59] as possible, changing only what is required to make the spacecraft non-nuclear. The PowerSail spacecraft configuration changes only the baseline propulsion system and, of course, replaces the RTG system. Importantly, the instrument size allocation and the science instruments themselves were unchanged in order to provide the same science return from the non-nuclear PowerSail spacecraft.

The PowerSail spacecraft configuration is shown in **Fig. 6**. It has a total height of 6.3m and fits well within a 4.5m envelope (Fig. 6a). The PowerSail subsystem is a 1x4.5m cylindrical stowage area in this configuration, which is deployed into a planar configuration once in space. The 'framed' stowage area is shown in Fig. 6a without the actual PowerSail blanket modeled. A Falcon Heavy shroud is being utilized (Fig. 6b), yielding no fit issues for the launch configuration. The propulsion bus has a basic 2x2 layout for the fuel/oxidizer tanks. The tanks are intended to be non-load bearing and supported within the load bearing structure. The tanks can be supported in multiple locations at the dome/cylinder interfaces. The deployable probe is side mounted between theses propulsion tanks.

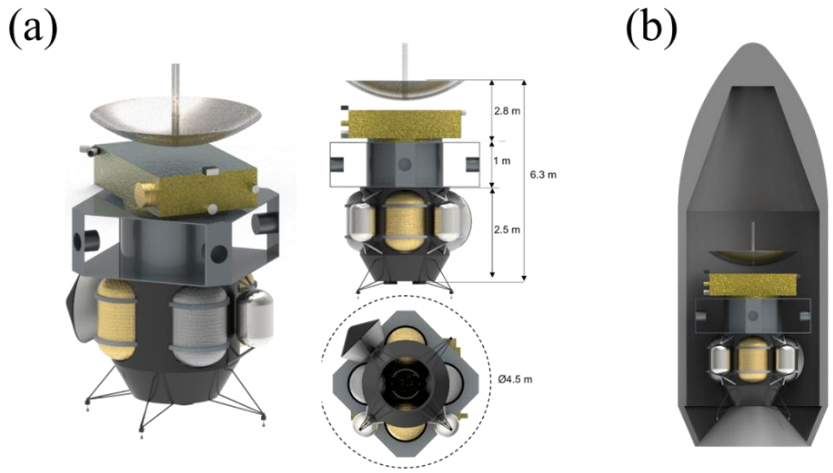

Fig. 6: Rendering of Uranus non-nuclear PowerSail spacecraft (a) dimensional retendering with PowerSail in stowed configuration and (b) stowed spacecraft in Falcon Heavy Shroud

C. Propulsion

The developed propulsion system is a pressure-fed Nitrogen Tetroxide (N2O4) Monomethyl hydrazine (MMH) bipropellant system as shown in **Fig. 7**. The system is sized for a maximum propellant capacity of ~4893kg of propellant (Table 2). The system employs two engine types: two R42 main engines and 16x R6F engines for attitude control. All four propellant tanks (two for N2O4 and two for MMH) are Northrop Grumman 80570-4 – currently in-production tanks. Because of their large size, two new high pressure (4500 psia) composite overwrapped pressure vessel (COPV) tanks will need to be designed for this non-nuclear solution system. The feed system is a standard pressure fed N2O4/MMH system.

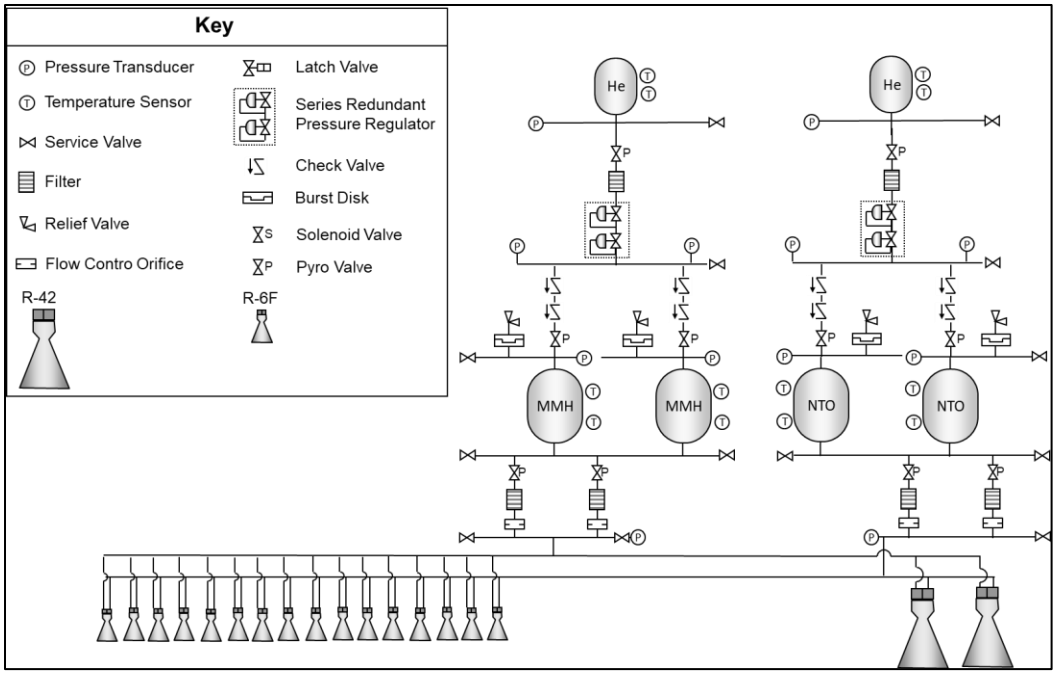

Fig. 7: N2O4/MMH Bipropellant Propulsion System Schematic.

The propulsion system was sized to meet the nuclear-bassline mission with an initial mass of 8340kg injected by the Falcon Heavy rocket and a total in-space ΔV of 2780m/sec. Both the main and ACS engines have an I_{sp} of 305s. Propellant residuals were assumed to be 2% which is consistent with the nuclear baseline. The propellant tank pressure was assumed to be 350psia with an ullage volume also at 2%. The pressurant system was assumed to have a max expected operating pressure (MEOP) of 4500psia and a temperature of 300K. The propulsion MEL is shown in **Table 3**.

Table 3: Propulsion Subsystem MEL

Mass Estimation List (MEL)			Qty	Unit Mass (kg)	Basic Mass (kg)	MGA (%)	MGA (kg)	Predicted Mass (kg)
2.0 Propulsion					**448.04**	**7.5%**	**33.59**	**481.63**
	2.1	R-42 NTO/MMH Engine	2	4.53	9.06	3.0%	0.27	9.33
	2.2	R-6F NTO/MMH Engine	16	0.97	15.44	3.0%	0.46	15.90
	2.3	Oxidizer (NTO) Tank	2	46.80	93.60	3.0%	2.81	96.41
	2.4	Fuel (MMH) Tank	2	46.80	93.60	3.0%	2.81	96.41
	2.5	Pressurant Tank	2	94.30	188.60	10.0%	18.86	207.46
	2.6	Propulsion Feed Components (valves, etc.)	1	6.88	6.88	3.0%	0.21	7.09
	2.7	Lines and Fittings	1	40.86	40.86	20.0%	8.17	49.03

D. Avionics

In the nuclear spacecraft design, the Avionics circuit boards are integrated into one Integrated Electronics Module (IEM). The IEM is fully redundant with a A side and B side, with cross-strapping of boards. Much of the Avionics is based on the Parker Solar Probe mission [60], and comm components based on the Europa Clipper mission [21]. For MSFC's non-nuclear configuration, modifications to the existing avionics, through modification of the IEM, is required (**Fig. 8**) to control the PowerSail deployment and to monitor the health and status of the PowerSail system. Modifications are also needed to regulate, switch, and otherwise distribute the potentially varying power load from the PowerSail. Two deployment controller boards are added to IEM to meet these requirements, where one board is for redundance to maintain the baseline fault tolerance. In addition, two remote interface units (RIUs), specific to data acquisition for monitoring of the PowerSail system, have also been added. Power distribution boards will be discussed below in the '*power'* subsection but are added to the IEM in replacement to current power management boards. Additionally, avionics cabling needed for the new control, monitoring, and regulation have been incorporated. Aluminum plating is used to provide a total of 250krad of total ionizing does (TID) protection for the electronics during the long, deep space mission.

For the communications system, a top-level analysis of the nuclear spacecraft design was done to verify its performance in meeting the non-nuclear mission downlink requirements. The same dual Ka/X-band 3.1m high gain antenna (HGA) is used for direct-to-Earth data link using 34m Deep Space Network (DSN) stations. Link budget analysis using 2.1GB/orbit data generated with a 70MB/day downlink at 8hrs/day DSN link time and a 19.5kbps data rate showed that the nuclear spacecraft communications system is sufficient for the PowerSail configuration. The additional telemetry data required for the PowerSail health and status was determined to be an insignificant addition and no change to the communications system is needed. This assumes 32GB of non-volatile memory for science and engineering telemetry data with appropriate compression schemes being employed. It is further assumed the data collection rate will not change for the longer 44-day orbits of the PowerSail configuration.

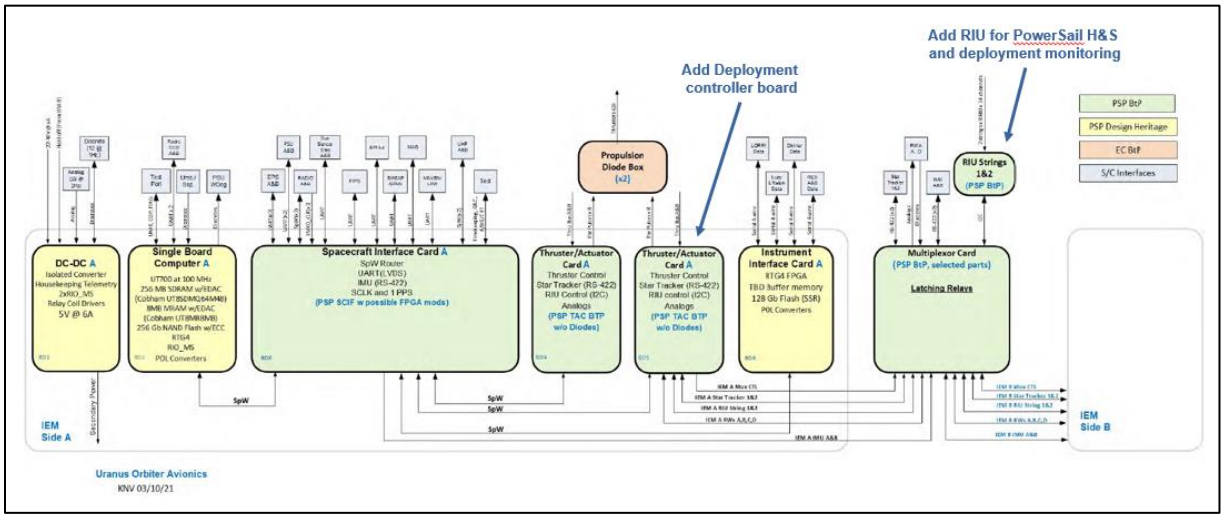

Fig. 8: Avionics Block Diagram

The additional board masses and power draws for the PowerSail deployment boards were based on that of the Thrust Actuator Cards and added to the IEM resource allocations (**Table 4**). Allocation for the new RIU's was also added. The RIUs will use the existing multiplexer interface board and data bus. The nuclear spacecraft design already has a significant mass for cabling (113 kg), which is based on historical planetary missions and was carried into the non-nuclear configuration with ~5% additional allocation for cabling to the new boards.

Table 4: Avionics & Comm MEL

IEM mass increase 1.4 kg for PowerSail deployment controller boards

Mass Estimation List (MEL)		Qty	Unit Mass (kg)	Basic Mass (kg)	MGA (%)	MGA (kg)	Predicted Mass (kg)
3.0 Avionics				**240.08**	**13.9%**	**33.32**	**273.40**
3.1	Integrated Electronics Module (IEM)	1	15.38	15.38	10.0%	1.54	16.92
3.2	Propulsion Diode Box (PDB)	4	3.18	12.72	10.0%	1.27	13.99
3.3	Remote Interface Unit (RIU)	18	0.09	1.62	10.0%	0.16	1.78
3.4	Communications	1	60.36	60.36	13.0%	7.85	68.21
3.5	Dish Antenna	1	32.00	32.00	15.0%	4.80	36.80
3.6	Harness	1	118.00	118.00	15.0%	17.70	135.70

2 additional RIU for PowerSail and deployment monitoring

Increase in cable mass 5kg for PowerSail deployment mechanism

E. Power

The power subsystem, like the all others, is based on the referenced nuclear configuration. Herein, the PowerSail solar array along with secondary energy storage replaces the RTG system and power management board updates are

made to regulate the varying amounts of power from the array, which is especially dependent on distance from the sun. Power distribution to the loads on the backend of the system remains largely consistent.

In total, the power system consists of the PowerSail itself, a secondary battery-based energy storage system, and power management and distribution system including electrical integration cabling to the spacecraft and payload loads. For this mission, a 765m^2 PowerSail configuration is baselined, between that of a NEAScout class and Solar Cruiser class sail. The PowerSail array is comprised of >28% efficient Inverted MetaMorphic (IMM) thin-film photovoltaic cells, each with integrated bypass diodes. The cells are bonded without adhesive to a substrate of 2-3µm thick colorless polyimide 1 (CP1). The cells are interconnected with thin-film silver foil to form strings. The silver is 'laminated' with a toughened version of CP1 stripes for environmental and electrostatic discharge protection. The cells are coated with a 50µm thick coating of Optinox polyimide for environmental protection [42], however, the performance of this coating in long, deep space exposure in currently unknown and likely in need of significant development. Alternatively, recent work by Kirmani et al. [61, 62] has shown that a 1-micron layer of vapor deposited silicon monoxide (SiO) added significant protection to a perovskite solar cell irradiated with 0.05MeV protons and 1MeV electrons. At a density of 2.1g/cc, this leads to an added mass of just 2.1g/m^2 of solar array and could be utilized at reasonable thicknesses. Copper ribbon, embedded into the backside of the CP1 substrate routes power from the strings to the spacecraft bus.

Table 5: Summary of the power requirements for each of the mission phases (in Watts)

Source	Launch	Cruise Checkout	Cruise Hibernation	Safe	Momentum Dump	Pre-Heat	DSM/UOI	Probe Ops	Tour Science	Radio Science	Downlink
Propulsion	0	0	0	0	28.2	0	200	0	0	0	0
Avionics	27	27	26.7	27	27	27	27	27	27	27	27
Electric Power	34.6	34.6	34.6	34.6	34.6	34.6	34.6	34.6	34.6	34.6	34.6
Attitude Determination & Control	0	124.8	0	98	98	98	98	98	98	98	98
Thermal	10.2	15	54	19.8	19.8	60	0	36	36	36	36
Communications	63.5	111.7	57.1	118.1	111.7	57.1	111.7	118.1	57.1	111.7	112.3
Spacecraft Totals	135.3	313.1	172.4	297.5	319.3	276.7	471.3	313.7	252.7	307.3	307.9
Science Payload	18.3	18.3	18.3	18.3	18.3	18.3	18.3	18.3	35.7	18.3	18.3
Harness Losses (3%)	4.6	9.9	5.7	9.5	10.1	8.9	14.7	10.0	8.7	9.8	9.8
Total Power	158.2	341.3	196.4	325.3	347.7	303.9	504.3	342.0	297.1	335.4	336.0
Growth (30%)	47.5	102.4	58.9	97.6	104.3	91.2	151.3	102.6	89.1	100.6	100.8
Predicted Power	**205.7**	**443.7**	**255.3**	**422.9**	**452.0**	**395.0**	**655.6**	**444.5**	**386.2**	**436.0**	**436.8**

The electrical power for each of the mission phases is provided by the PowerSail array, except for the "Launch" and "DSM/UOI" (Deep Space Maneuver / Uranus Orbit Insertion) Phases (**Table 5**). These phases are powered by the secondary battery bank. As can be seen from the predicted power load, the "Momentum Dump" phase requirement sizes the PowerSail array at 452W, while the "DSM/UOI" phase power requirement sizes the energy storage subsystem at 655.6W.

Table 6: Key design points and assumptions used for sizing the PowerSail array and supporting battery:

Property	Value	Notes
Provision	Regulated bus power to spacecraft and science payload	
Bus Voltage	28V	
Powersail Array Voltage	200V	
PowerSail Substrate Areal Density	4.62 g/m^2	
PowerSail Coating Areal Density	26.25 g/m^2	
PV Cell Areal Density	250 g/m^2	
PV Cell Min Temperature	80K	
PV Cell Conversion Efficiency	28%	Minimum at operating temp (80K - 350K) and 4 W/m^2 irradiance
PV Cell Coverage	93%	% array covered in PV Cells
Initial Array Power Knockdown	18%	for deployment damage, curvature, coating
Solar Irradiance (AM0)	1366.1 W/m^2	
PowerSail Mass Growth Allowance	50%	
Secondary Battery Reference Cell	LG INR18650 MJ1	
Secondary Battery Cell Ampacity	3.25 Ahr	Minimum
Secondary Battery Packing Factor	1.3	
Power cable conductor Sizing Loss	1%	

Table 6 summarizes the key design points and assumptions utilized to size both the PowerSail solar array as well as the secondary supporting battery system. The initial array derating includes all the knockdown factors for the PowerSail array as a single de-rate. This includes expected slight curvatures in the deployed sail, small tears and damage induced during deployment, as well as manufacturing defects for assembling a large thin-film array. The PV conversion efficiency represents the end-of-life minimum at low intensity low temperature (LILT) operation. The PowerSail sized for this application is 765 m^2 and has a predicted mass of 498kg. The PV cells must be capable of producing >450W of power near Earth without incurring damage while then achieving the same power generation at >28% conversion efficiency near Uranus where the irradiance is just ~3.7W/m^2[19] and the cell surface temperature is as low as 78k. Conceptually, the PowerSail will be partially deployed near Earth to expose a fraction of the power generating capability and incrementally deployed as the PowerSail travels deeper into space. For example, ~0.25% deployed near Earth (Solar Constant=1 [19]), ~10% deployed by Jupiter (Solar Constant=0.03695 [19]), ~25% deployed by Saturn (Solar Constant=0.01099 [19]), and 100% deployed by Uranus (Solar Constant=0.002718 [19]). This incremental deployment also keeps voltage and current at reasonable levels; thereby, keeping copper conductor mass lower, simplifying power management board deigns and limiting sustained arc risk [63]. The electrical configuration to enable this configuration along with, and more importantly, the LILT solar cell operation at Uranus remains one of the biggest challenges to making the PowerSail a reality.

The reference cell for the secondary battery (LG INR18650 MJ1) was selected because it is a well-tested, high specific-energy cell in general use in the industry. The batteries must survive an 18.5-year journey through deep space – a very long life for any Li-Ion battery system. For this reason, a fully redundant 8s16p battery is baselined, however, this marks a second critical area of development needed in the path to reality. The complete mass breakdown for the power subsystem is given in **Table 7**.

Table 7: Power subsystem MEL breakdown

Mass Estimation List (MEL)			Qty	Unit Mass (kg)	Basic Mass (kg)	MGA (%)	MGA (kg)	Predicted Mass (kg)
5.0 Power					**446.70**	**38.5%**	**172.07**	**618.77**
	5.1	PowerSail	1	238.90	238.90	50.0%	119.45	358.35
	5.2	PowerSail Deployer	1	53.20	53.20	30.0%	15.96	69.16
	5.3	PowerSail Booms	4	13.50	54.00	30.0%	16.20	70.20
	5.4	Harness	1	12.80	12.80	50.0%	6.40	19.20
	5.5	Array Reg / Battery Charge Ctl	1	26.40	26.40	30.0%	7.92	34.32
	5.6	Power Switching Unit	2	22.50	45.00	10.0%	4.50	49.50
	5.7	Battery	2	8.20	16.40	10.0%	1.64	18.04

F. Guidance, Navigation, and Control

The attitude control design of PowerSail spacecraft combines a structure that is similar in size and structural properties to a solar sail, with higher inertia and a traditional mass bus. The conceptual design focused on sizing and selection of attitude control hardware. The result being a design that accommodated the large PowerSail inertia, and its disturbance torques using traditional control actuators and sensors on the spacecraft bus. The low frequency structural modes of a large gossamer structure drives lower slew rates on a solar sail, so control actuators designed for high slew rates on a traditional spacecraft work for PowerSail [64]. The science tracking rate was assumed to be 0.024deg/s pitch with 9.1e-6deg/s^2 angular acceleration. These values allow the spacecraft to track the velocity vector of the spacecraft at its closest approach to Uranus and highest rotation rate. The science instruments are assumed to provide any additional tracking rates to follow their targets. The rates were limited to accommodate the large, gossamer PowerSail array. The attitude performance required for the science payload is 0.06 deg per axis while the sail is pointing inertially and during science slews. This accuracy supports both science observations and communications back to Earth.

The center of mass to center of pressure offset is assumed to be limited to 5cm to accommodate uncertainties in the relation between the sail shape and spacecraft bus. This is based on experience with the Solar Cruiser sail and control system design. The PowerSail fully deployed size was assumed to be 35m on a side, with 1225m^2 total area – conservatively much larger than what is needed to close the mission power profile to ensure significant growth allowance and safety factor on the essential GNC components. A trade study was performed on using a partially deployed sail from Earth to Jupiter flyby per the power generation scheme to incrementally deploy and expose power generating cells. A 10% deployed width was assumed for this analysis.

There is sufficient heritage control system hardware that have demonstrated the performance and lifetime in deep space to meet the needs of PowerSail. Reaction wheels control the attitude throughout the mission. Star trackers provide attitude determination and rates after PowerSail deployment. IMUs provide rate information before sail deployment. Sun sensors provide robust sun pointing on initialization of the spacecraft and during safe modes. The propulsion system includes RCS thrusters that provide detumble during spacecraft initialization, control during propulsive maneuvers, backup attitude control to the reaction wheels, and momentum management throughout the mission. The momentum accumulation by the PowerSail over the entire trajectory from Earth to Uranus is small enough that the propellant required by the RCS thrusters is minimal (~4 kg) compared to the total propellant budget, due to the large propulsive maneuvers required for the size of the bus. From a momentum management perspective, there is little advantage to wait to fully deploy the PowerSail until farther from the sun and, thus, can be deployed as needed per power generation requirements.

To support the science tracking rate, a pyramid of reaction wheels with ~2.2 Newton-meter-seconds oriented 60 degrees off the normal vector of the PowerSail are required. Larger wheels than this do not add appreciably to the mass and provide ample margin to support inertia growth of the sail or increased momentum capacity if a more detailed control design finds the system can support faster slews.

More detailed science pointing, and rate requirements and the limitations imposed by the large, flexible PowerSail will drive many aspects of the control system and spacecraft design. If rates and pointing are incompatible with pointing the sail, then instrument pointing may be required. Flexible modes of the sail will limit the slew rate of the control system. The power budget will limit how far away from the sun the sail can be allowed to point. The GN&C subsystem MEL is shown in **Table 8**.

Table 8: GN&C Subsystem MEL

Mass Estimation List (MEL)			Qty	Unit Mass (kg)	Basic Mass (kg)	MGA (%)	MGA (kg)	Predicted Mass (kg)
4.0 GN&C					**71.40**	**5.0%**	**3.54**	**74.94**
	4.1	Star Tracker - Sensor head	3	1.40	4.20	3.0%	0.13	4.33
	4.2	Star Tracker - Electronic Unit	2	1.80	3.60	3.0%	0.11	3.71
	4.3	SIRU	1	7.10	7.10	3.0%	0.21	7.31
	4.4	Digital Sun Sensor - Sensor Head	5	0.30	1.50	3.0%	0.05	1.55
	4.5	Digital Sun Sensor - Electronics Unit	1	1.00	1.00	3.0%	0.03	1.03
	4.6	Reation Wheel Assembly	4	8.50	34.00	3.0%	1.02	35.02
	4.7	Radiation Shielding	1	20.00	20.00	10.0%	2.00	22.00

G. Structures

The MSFC defined spacecraft BUS and PowerSail is a new design when compared to the APL nuclear mission. The MSFC design houses two NTO tanks and two MMH tanks for the MPS/RCS thrusters along with press tanks to pressurize the propellant tanks. This differs from the nuclear design which used a nested NTO and MMH propellant tank with a common bulkhead and, of course, did not have the PowerSail array. Both APL and MSFC designs provide the same subsystem support required to meet the science mission objectives, but they have very different structural design layouts.

The structural analysis requires sizing of the four PowerSail booms and spacecraft BUS with all subsystem mass included in the analysis FEM. PowerSail booms must be able to meet strength and deflection requirements during propulsive events with the PowerSail deployed. The primary structure was sized to meet requirements per NASA STD-5001B and Falcon Heavy launch loads (6g Axial, 2g Lateral) were assumed. A proto-flight design approach for metal structures (FSu=1.4, FSy=1.25) was used with FSu=2.0 for composite structures and an aluminum spacecraft construction. The PowerSail boom construction was assumed to be a MR60H Unidirectional Tape, T300 Plain Weave Fabric composite; which is the same materials used on MSFC ‘Cruiser Class‘ solar sail designs [65]. The MPS tanks are not considered part of the primary load path.

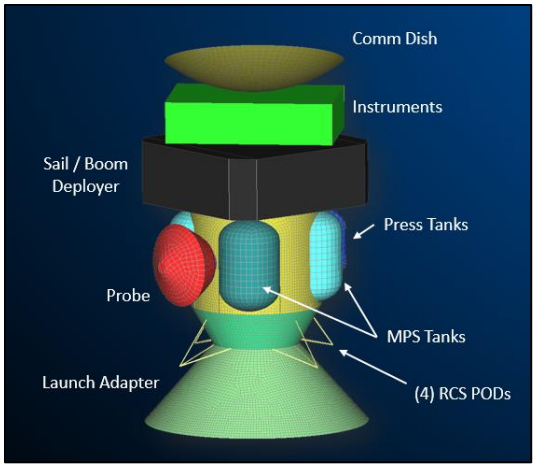

Fig. 9: **Model 1 FEM (Spacecraft BUS with Stowed PowerSail and Instruments)**

Three Models were created to analyze the PowerSail structures as follows: Model 1 Spacecraft BUS (**Fig. 9**) – A finite element model was created to size the spacecraft BUS which houses MPS tanks, Press tanks, RCS PODs, and MPS thrusters. Forward mounted subsystems include a Solar Array Sail deployer as well as instruments which are included in an Instrument containment box. Additionally, there is a communications dish antenna mounted on top of the Instrument/subsystem box. Subsystems mounted in the instrument box include Avionics, Power, Thermal, GN&C, etc.

Model 2 PowerSail Boom Loads Model (**Fig. 10**) – A finite element model was developed to aid in Boom load input definitions. It is assumed that each sail quadrant attaches to the booms five locations along the length of each boom as shown in the Fig. below. Assuming a worst-case propulsive maneuver case (Uranus Orbit Insertion), the finite element model was run using inertia relief with a 400lbf thrust load applied at the thruster locations. Boom input loads were then extracted from the Nastran results file for use in evaluating a boom model meshed using CQUAD4 shell elements.

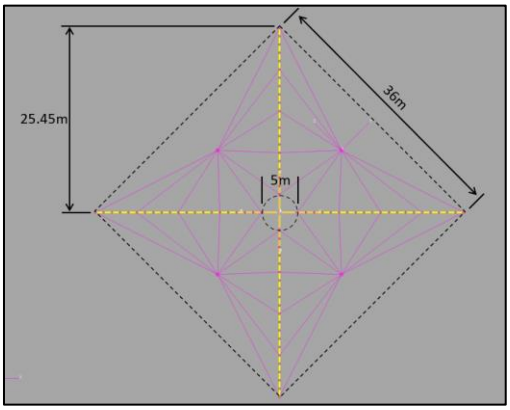

Fig. 10: Model 2 FEM Solar Array Sail Boom Loads Model

Model 3 Boom sizing FEM (**Fig. 11**) – A second Boom model was developed to size the composite boom structure which must meet strength and deflection requirements. Analysis indicates that the critical failure criteria is boom deflection which was limited to 40 inches at the tip of each boom using engineering judgement.

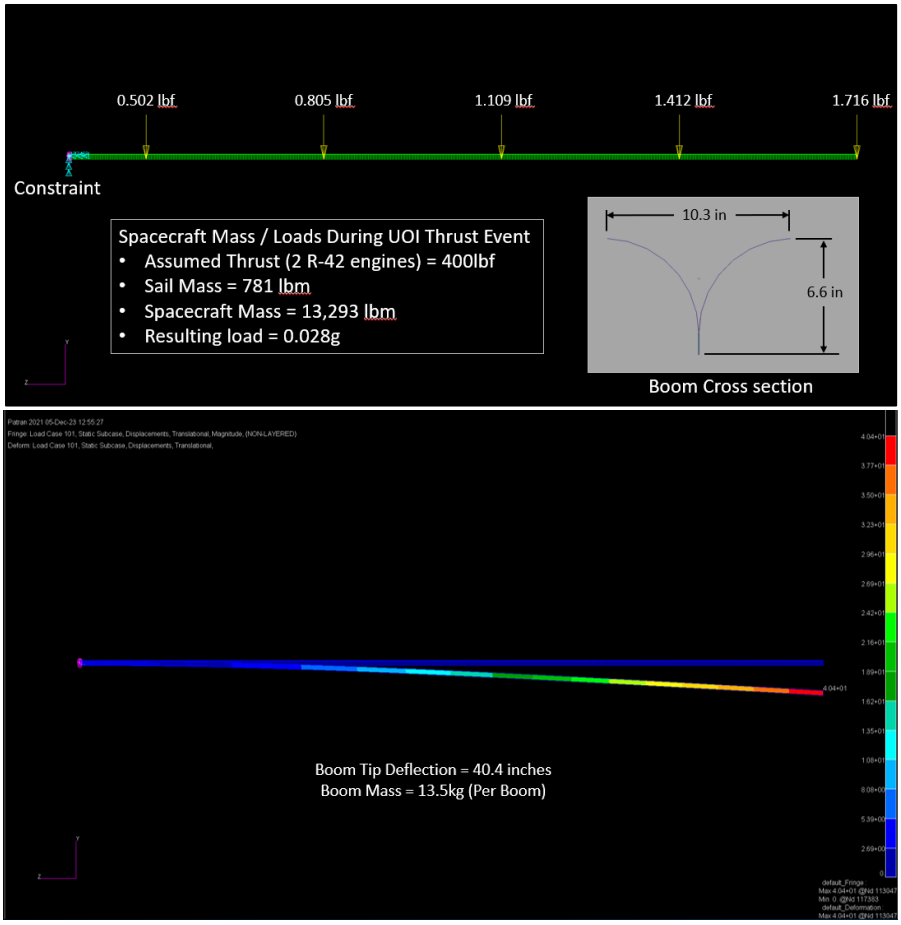

Fig. 11: Model 3 Boom sizing FEM

All spacecraft BUS structures meet or exceed strength / stability requirements per NASA STD-5001B for the launch / ascent load cases evaluated. The PowerSail Boom structures met strength requirements per NASA STD-5001B. Boom tip deflection was limited to 40 inches during UOI. Note that a tip deflection limit was set using engineering judgement in lieu of any other requirements information. Mass and CG were well within limits of the Falcon Heavy requirement of 4m (**Fig. 12**). **Table 9** shows the structures subsystem MEL.

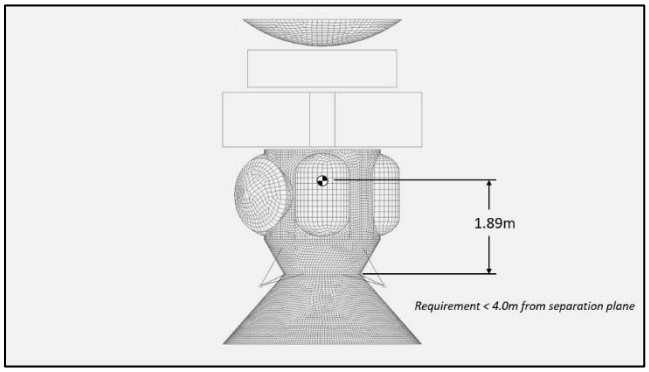

Fig. 12: PowerSai Spacecraft Mass / CG

Table 9: Spacecraft BUS Structures MEL

Mass Estimation List (MEL)			Qty	Unit Mass (kg)	Basic Mass (kg)	MGA (%)	MGA (kg)	Predicted Mass (kg)
1.0 Structures					477.05	20.0%	95.41	572.46
	1.1	BUS Primary Structure	1	256.98	256.98	20.0%	51.40	308.38
	1.2	Instrument Containment Box	1	137.07	137.07	20.0%	27.41	164.48
	1.3	MPS Tank Support Structure	1	22.4	22.40	20.0%	4.48	26.88
	1.4	RCS Truss Members	1	2.09	2.09	20.0%	0.42	2.51
	1.5	MPS Tank upper Truss Supports	1	1.06	1.06	20.0%	0.21	1.27
	1.6	Truss Joints and Fittings	1	1.57	1.57	20.0%	0.31	1.89
	1.7	Secondary Structures	1	55.88	55.88	20.0%	11.18	67.05

H. Thermal

The thermal subsystem must keep all components within their allowable operational, survival, and storage temperature ranges during all mission phases. There are several distinct thermal regions on the spacecraft as shown in **Fig. 13**. The deployed PowerSail itself is considered region E and is not shown.

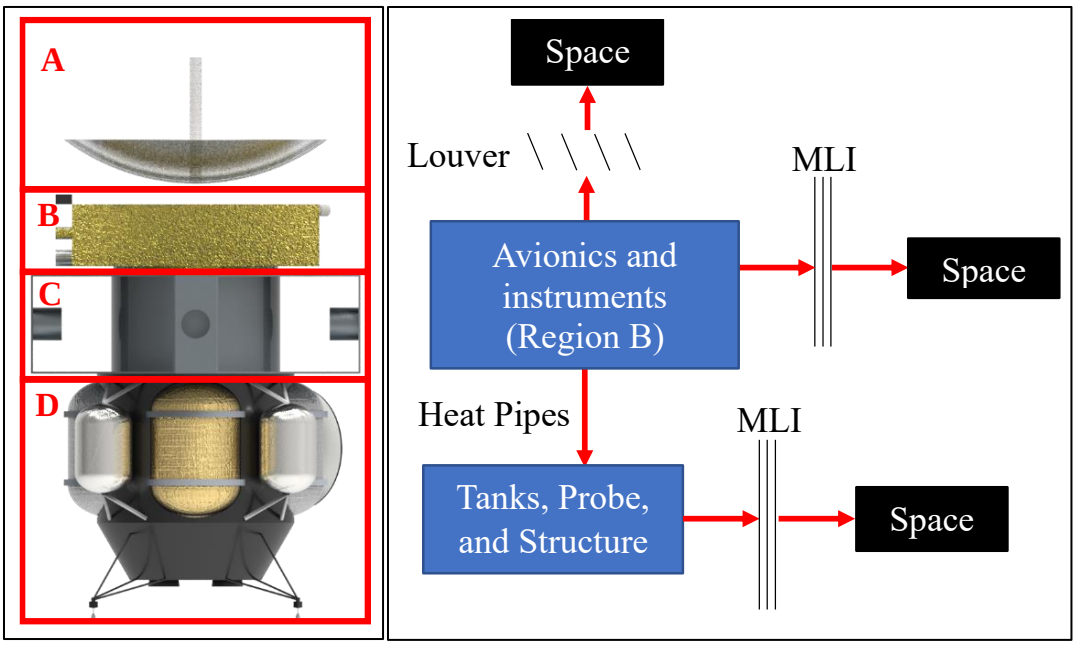

Fig. 13: Thermal Regions (Left) and Heat Map (Right)

Region A includes the high gain antenna which survived passively in the nuclear spacecraft design and is believed to be capable of this in the nonnuclear mission. Modeling indicates the high gain antenna would be close to room temperature near Earth and ~100 K near Uranus. Antennas can generally survive a very wide temperature range, so this conclusion was accepted as an assumption for this study.

Region B is the instrument, avionics, and power system section. It is insulated from the environment with MLI and radiatively cooled. A louver system is placed on the radiator, so the radiator's heat rejection can be turned down by 6x (this turndown ratio has been demonstrated through test) to reduce the radiative cooling near Uranus while still providing ample cooling near Earth. Waste heat from Region B is also used to prevent the propellant in Region D from freezing.

Region C is the stowed PowerSail and subsystem hardware. The PowerSail system electronics are in Region B, so none of the hardware in Region C needs to survive after PowerSail deployment. The PowerSail deploys incrementally near Earth, again between Earth and Jupiter, between Jupiter and Saturn, and finally fully by Uranus. Region C's thermal needs are limited to keeping motors and mechanism within survivability and operation temperatures appropriately. It is believed that components in Region C can be thermally managed with the addition of heaters and MLI without significantly affecting the overall system design.

Region D includes the propellant tanks, probe, and structure. Structure can be designed to have a very wide temperature range that survives to below Uranus temperatures and above near-Earth temperatures, so the thermal accommodations for structure will be inconsequential. The propellant in the tanks could freeze if they get too cold (analysis assumed 2 C limit, but propellant changed to allow for lower temperatures), and the probe was assumed to have a minimum temperature of -40 C. In the nuclear design, the propellant tanks were kept warm with waste heat from the radioisotope generator. In this design, the propellant tanks are kept warm with waste heat from the Region B. The waste heat is transported from Region B to Region D using passive heat pipes that are routed through Region C but insulated from Region C.

Three cases were considered for the thermal analysis: 1) near Earth during momentum dumping (452.0 W waste heat), 2) near Uranus during a deep space maneuver (655.6 W waste heat), and 3) near Uranus during science operations (386.2 W waste heat). The Thermal Desktop results for the bus and PowerSail are shown in **Fig. 14**.

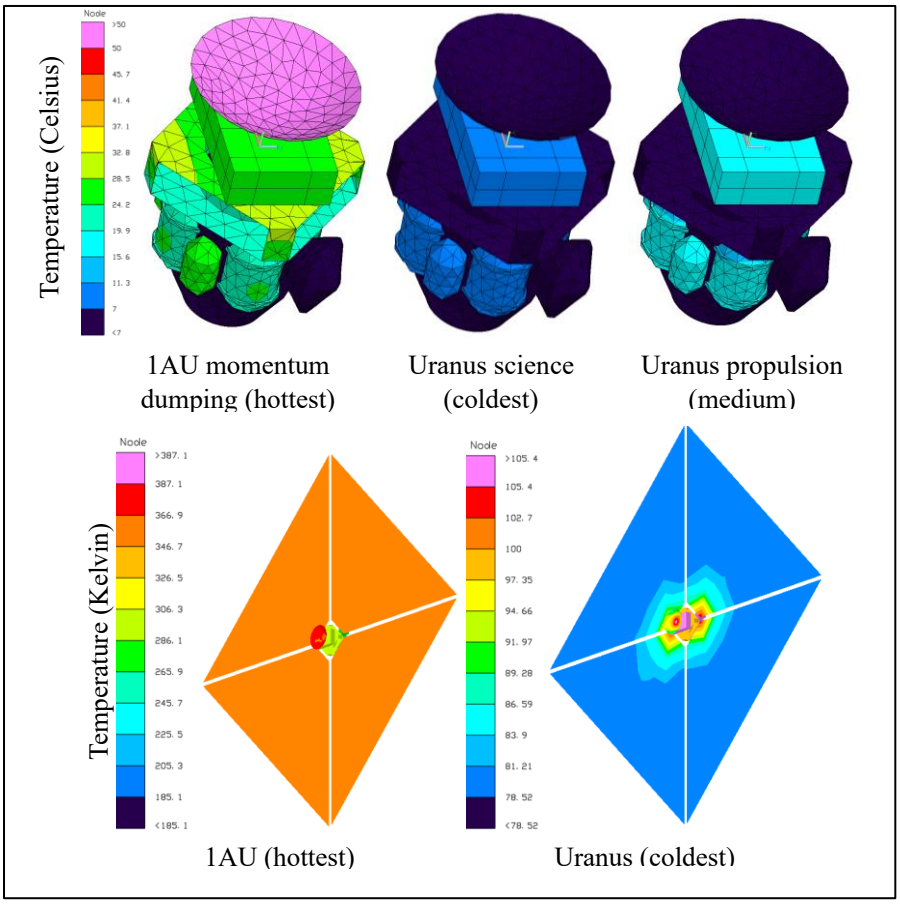

Fig. 14: Thermal Desktop Temperature Contours

There are several key findings from the analysis.

1. The avionics and instruments area (Region B) and the tanks and probe (Region D) can be maintained at acceptable temperatures through the three bounding cases considered by analysis.
2. The waste heat from the avionics is sufficient to keep the propellant tanks and probe warm with 16 aluminum-ammonia constant conductance heat pipes transferring the heat.
3. The PowerSail must be capable of surviving and operating from 78 K to 363 K (-195 C to 90 C).
4. The louver/radiator system can turn down enough to compensate for the difference between Earth's thermal environment and Uranus' thermal environment.

The masses for the conceptual thermal design were estimated and are shown in **Table 10**Table 10: Thermal Subsystem MEL. Around 90% of the mass comes from the MLI that covers the tanks and electronics.

Table 10: Thermal Subsystem MEL

Mass Estimation List (MEL)			Qty	Unit Mass (kg)	Basic Mass (kg)	MGA (%)	MGA (kg)	Predicted Mass (kg)
6.0 Thermal					**99.36**	**35.0%**	**34.78**	**134.13**
	6.1	20-layer MLI blankets (83 m2)	1	89.80	89.80	35.0%	31.43	121.23
	6.2	Insulating Spacers	8	0.01	0.08	35.0%	0.03	0.11
	6.3	Heaters, wiring, and thermostats	1	1.77	1.77	35.0%	0.62	2.40
	6.4	Louvers	4	1.00	4.00	35.0%	1.40	5.40
	6.5	Heat Pipes	16	0.17	2.70	35.0%	0.95	3.65
	6.6	Paint/Coatings	1	1.00	1.00	35.0%	0.35	1.35

Additional spreadsheet-level trades were performed to assess an idea of material checkerboarding the PowerSail (depicted in **Fig. 15**) to control its composite optical properties and consequently its temperature at Uranus – i.e. to increase the low side (78k) operating temperature. For this analysis, the solar cells were assumed to have an absorptivity of ~0.659 and an emissivity of ~0.917, and a second coating was added in place of solar cells per the checkerboard shown in Fig. 15 left. This coating is the GSFC Dark Mirror Coating SiO-Cr-Al which has an absorptivity of 0.86 and an emissivity of 0.04. The back side of the PowerSail was taken to be aluminum coated (emissivity of 0.03). Checkerboarding can be used to increase the temperature at Uranus but has the unfortunate side effect of increasing the PowerSail area for a given power requirement. The relationship between these two effects is shown in a graph in Fig. 15 right. The "Power Sail Area Multiplier" is the multiple which the PowerSail would have to increase in size to get the same amount of power with the incorporation of the optical squares. For example, at a Power Sail Area Multiplier of 2, the PowerSail would have to be twice as large to produce the same power as a PowerSail that hasn't been checkerboarded. Another issue with this concept is the heat conduction between the squares of the checkboard. It may be (depending on the PowerSail thickness) that the squares can only be ~0.5 mm thick for the PowerSail to be essentially isothermal. Alternative strips of coating and solar cells could be more convenient than patches. The near-Earth PowerSail temperatures can be decreased by rotating the PowerSail to reduce its solar projected area.

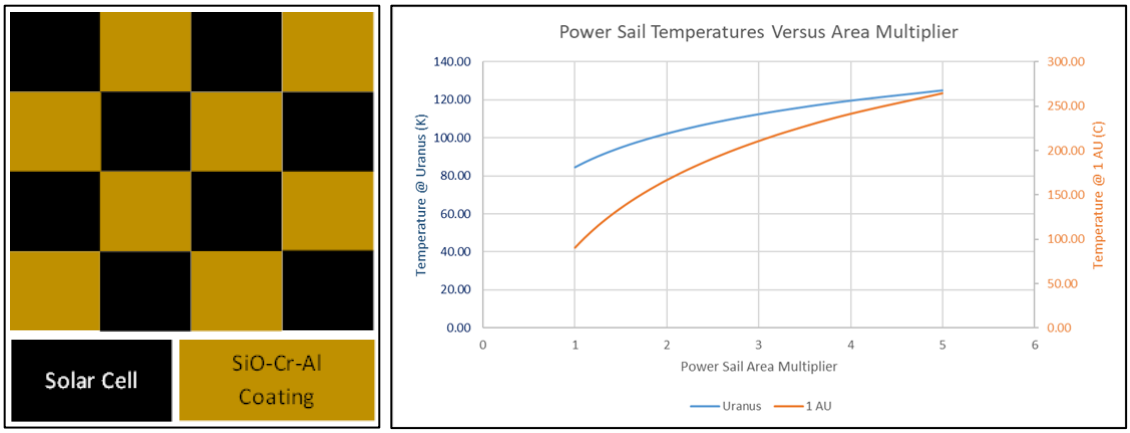

Fig. 15: Checkerboarding Concept (Left) and Power Sail Temperatures vs. Area Multiplier (Right)

IV. Conclusions and Comments Towards Reality

The PowerSail is a potentially disruptive power generation technology that could extend the range of non-nuclear spacecraft to extremely deep locations within our solar system. This is important to the science community as it could enable important missions without dependence on the scarce and expensive plutonium-238. A hypothetical non-nuclear, PowerSail based mission to Uranus, based on APL's Uranus Probe and Explorer, was studied. It was found that PowerSail spacecraft design could close the mission – meeting mass requirements for a Falcon Heavy launch, having the ability to be captured into Uranus orbit, and closing the thermal profile without the nuclear source waste heat. The PowerSail itself requires significant technology maturation to make this mission a reality. The PowerSail

deployment methodology and equipment must be developed. While based on heritage solar sail technology, significant update is expected to incorporate the solar cells, the electrical power wiring, as well as the incremental deployment through Uranus. PV cells, such as LILT IMM or LILT Perovskite, with >28% end-of-life conversion efficiency near Uranus must be devised. Advanced cover-materials to protect these cells from radiation and other environmental factors over the very long operation life must also be developed. Manufacturing techniques to reliably produce such a large, thin-film array is need. And lightweight battery cells must be designed and tested to near 20-year operation life.

Acknowledgments

This work was supported by the National Aeronautics and Space Administration's Marshall Space Flight Center's Internal Research and Development fund.

References

[1] Board, S. S., and Council, N. R. *Vision and voyages for planetary science in the decade 2013-2022*: National Academies Press, 2012.

[2] National Academies of Sciences, E., and Medicine. "Origins, worlds, and life: a decadal strategy for planetary science and astrobiology 2023-2032," 2022. doi: https://doi.org/10.17226/26522

[3] Arridge, C. S., Achilleos, N., Agarwal, J., Agnor, C., Ambrosi, R., André, N., Badman, S. V., Baines, K., Banfield, D., and Barthélémy, M. "The science case for an orbital mission to Uranus: exploring the origins and evolution of ice giant planets," *Planetary and Space Science* Vol. 104, 2014, pp. 122-140. doi: https://doi.org/10.1016/j.pss.2014.08.009

[4] Fletcher, L. N., Helled, R., Roussos, E., Jones, G., Charnoz, S., André, N., Andrews, D., Bannister, M., Bunce, E., and Cavalié, T. "Ice Giant Systems: The scientific potential of orbital missions to Uranus and Neptune," *Planetary and Space Science* Vol. 191, 2020, p. 105030. doi: https://doi.org/10.1016/j.pss.2020.105030

[5] Mousis, O., Atkinson, D. H., Cavalié, T., Fletcher, L., Amato, M., Aslam, S., Ferri, F., Renard, J.-B., Spilker, T., and Venkatapathy, E. "Scientific rationale for Uranus and Neptune in situ explorations," *Planetary and Space Science* Vol. 155, 2018, pp. 12-40. doi: https://doi.org/10.1016/j.pss.2017.10.005

[6] Cohen, I. J., Beddingfield, C., Chancia, R., DiBraccio, G., Hedman, M., MacKenzie, S., Mauk, B., Sayanagi, K. M., Soderlund, K. M., and Turtle, E. "The case for a new frontiers–class Uranus orbiter: system science at an underexplored and unique world with a mid-scale mission," *The planetary science journal* Vol. 3, No. 3, 2022, p. 58. doi: 10.3847/PSJ/ac5113

[7] Jarmak, S., Leonard, E., Akins, A., Dahl, E., Cremons, D., Cofield, S., Curtis, A., Dong, C., Dunham, E., and Journaux, B. "QUEST: A New Frontiers Uranus orbiter mission concept study," *Acta Astronautica* Vol. 170, 2020, pp. 6-26.

[8] Turrini, D., Politi, R., Peron, R., Grassi, D., Plainaki, C., Barbieri, M., Lucchesi, D. M., Magni, G., Altieri, F., and Cottini, V. "The ODINUS Mission Concept-The Scientific Case for a Mission to the Ice Giant Planets with Twin Spacecraft to Unveil the History of our Solar System," *arXiv preprint arXiv:1402.2472*, 2014.

[9] Bennett, G. L. "Radioisotope Power: Technology Options," *Encyclopedia of Nuclear Energy*. Elsevier Oxford, 2021, pp. 191-200.

[10] Bennett, G., Lombardo, J., and Rock, B. "US radioisotope thermoelectric generators in space," *Nuclear Engineer* Vol. 25, No. 2, 1984, pp. 49-58.

[11] Bennett, G. L., and Skrabek, E. "Power performance of US space radioisotope thermoelectric generators," *Fifteenth International Conference on Thermoelectrics. Proceedings ICT'96*. IEEE, 1996, pp. 357-372.

[12] Werner, J. E., Johnson, S. G., Dwight, C. C., and Lively, K. L. "Cost Comparison in 2015 Dollars for Radioisotope Power Systems--Cassini and Mars Science Laboratory." Idaho National Lab.(INL), Idaho Falls, ID (United States), 2016.

[13] Council, N. R., Engineering, D. o., Sciences, P., Aeronautics, Board, S. E., Board, S. S., and Committee, R. P. S. *Radioisotope power systems: an imperative for maintaining US leadership in space exploration*: National Academies Press, 2009.

[14] Daily, C. R., and McDuffee, J. L. "Design studies for the optimization of 238Pu production in NpO2 targets irradiated at the High Flux Isotope Reactor," *Nuclear Technology* Vol. 206, No. 8, 2020, pp. 1182-1194. doi: https://doi.org/10.1080/00295450.2019.1674594

[15] Witze, A. "Desperately seeking plutonium," *Nature* Vol. 515, No. 7528, 2014, p. 484. doi: https://doi.org/10.1038/515484a

[16] Wham, R., Onuschak, B., and Sutliff, T. "Plutonium-238 supply project—Additional processing enabling power for future NASA missions," *2016 IEEE Aerospace Conference*. IEEE, 2016, pp. 1-9.
[17] Depaoli, D. W., Benker, D., Delmau, L. H., Sherman, S. R., Riley Jr, F., Bailey, P. D., Collins, E. D., and Wham, R. M. "Process development for plutonium-238 production at Oak Ridge National laboratory." Oak Ridge National Lab.(ORNL), Oak Ridge, TN (United States), 2019.
[18] Collins, E. D., Morris, R. N., McDuffee, J. L., Mulligan, P. L., Delashmitt, J. S., Sherman, S. R., Vedder, R. J., and Wham, R. M. "Plutonium-238 production program results, implications, and projections from irradiation and examination of initial NpO2 test targets for improved production," *Nuclear Technology* Vol. 208, No. sup1, 2022, pp. S18-S25. doi: : 10.1080/00295450.2021.2021769
[19] Rauschenbach, H. S. *Solar cell array design handbook: the principles and technology of photovoltaic energy conversion*: Springer Science & Business Media, 2012.
[20] Matousek, S. "The Juno new frontiers mission," *Acta Astronautica* Vol. 61, No. 10, 2007, pp. 932-939. doi: https://doi.org/10.1016/j.actaastro.2006.12.013
[21] Bayer, T., Bittner, M., Buffington, B., Dubos, G., Ferguson, E., Harris, I., Jackson, M., Lee, G., Lewis, K., and Kastner, J. "Europa clipper mission: Preliminary design report," *2019 IEEE aerospace conference*. IEEE, 2019, pp. 1-24.
[22] Roberts, J. H., McKinnon, W. B., Elder, C. M., Tobie, G., Biersteker, J. B., Young, D., Park, R. S., Steinbrügge, G., Nimmo, F., and Howell, S. M. "Exploring the interior of Europa with the Europa Clipper," *Space Science Reviews* Vol. 219, No. 6, 2023, p. 46.
[23] Johnson, L., Whorton, M., Heaton, A., Pinson, R., Laue, G., and Adams, C. "NanoSail-D: A solar sail demonstration mission," *Acta astronautica* Vol. 68, No. 5-6, 2011, pp. 571-575. doi: https://doi.org/10.1016/j.actaastro.2010.02.008
[24] Johnson, L., Young, R., Montgomery, E., and Alhorn, D. "Status of solar sail technology within NASA," *Advances in Space Research* Vol. 48, No. 11, 2011, pp. 1687-1694. doi: https://doi.org/10.1016/j.asr.2010.12.011
[25] Tsuda, Y., Mori, O., Funase, R., Sawada, H., Yamamoto, T., Saiki, T., Endo, T., and Kawaguchi, J. i. "Flight status of IKAROS deep space solar sail demonstrator," *Acta astronautica* Vol. 69, No. 9-10, 2011, pp. 833-840.
[26] Johnson, L., Castillo-Rogez, J., and Dervan, J. "Near Earth Asteroid Scout: NASA's Solar Sail Mission to a NEA." NTRS 20170009096, NASA Technical Report, 2017.
[27] Wilkie, W. K. "Overview of the nasa advanced composite solar sail system (acs3) technology demonstration project," *AIAA Scitech 2021 Forum*. 2021, p. 1260.
[28] Johnson, L., Everett, J., McKenzie, D., Tyler, D., Wallace, D., Newmark, J., Turse, D., Cannella, M., Wilson, J., and Feldman, M. "The NASA Solar Cruiser Mission-Solar Sail Propulsion Enabling Heliophysics Missions," 2022.
[29] Spencer, D. A., Betts, B., Bellardo, J. M., Diaz, A., Plante, B., and Mansell, J. R. "The LightSail 2 solar sailing technology demonstration," *Advances in Space Research* Vol. 67, No. 9, 2021, pp. 2878-2889.
[30] Schermer, J., Mulder, P., Bauhuis, G., Larsen, P., Oomen, G., and Bongers, E. "Thin-film GaAs epitaxial lift-off solar cells for space applications," *Progress in Photovoltaics: Research and Applications* Vol. 13, No. 7, 2005, pp. 587-596. doi: https://doi.org/10.1002/pip.616
[31] Otte, K., Makhova, L., Braun, A., and Konovalov, I. "Flexible Cu (In, Ga) Se2 thin-film solar cells for space application," *Thin Solid Films* Vol. 511, 2006, pp. 613-622. doi: https://doi.org/10.1016/j.tsf.2005.11.068
[32] Gupta, V., Cruz-Campa, J. L., Okandan, M., and Nielson, G. N. "Microsystems-enabled photovoltaics: A path to the widespread harnessing of solar energy," *Future Photovoltaics* Vol. 1, No. 1, 2010, pp. 28-36.
[33] Nielson, G. N., Okandan, M., Cruz-Campa, J. L., Resnick, P. J., Wanlass, M. W., Clews, P. J., Pluym, T. C., Sanchez, C. A., and Gupta, V. P. "Microfabrication of microsystem-enabled photovoltaic (MEPV) cells," *Advanced Fabrication Technologies for Micro/Nano Optics and Photonics IV*. Vol. 7927, International Society for Optics and Photonics, 2011, p. 79270P.
[34] Cornfeld, A., and Stan, M. A. "Inverted metamorphic multijunction solar cells." Vol. 8,536,445, U.S. Patent, 2013.
[35] Kayes, B. M., Zhang, L., Twist, R., Ding, I.-K., and Higashi, G. S. "Flexible thin-film tandem solar cells with> 30% efficiency," *IEEE Journal of Photovoltaics* Vol. 4, No. 2, 2014, pp. 729-733. doi: http://dx.doi.org/10.1109/JPHOTOV.2014.2299395
[36] Cardinaletti, I., Vangerven, T., Nagels, S., Cornelissen, R., Schreurs, D., Hruby, J., Vodnik, J., Devisscher, D., Kesters, J., and D'Haen, J. "Organic and perovskite solar cells for space applications," *Solar Energy Materials and Solar Cells* Vol. 182, 2018, pp. 121-127. doi: https://doi.org/10.1016/j.solmat.2018.03.024

[37] Kirk, A., Cardwell, D., Wood, J., Wibowo, A., Forghani, K., Rowell, D., Pan, N., and Osowski, M. "Recent progress in epitaxial lift-off solar cells," *2018 IEEE 7th World Conference on Photovoltaic Energy Conversion (WCPEC)(A Joint Conference of 45th IEEE PVSC, 28th PVSEC & 34th EU PVSEC)*. IEEE, Waikoloa, HI, 2018, pp. 0032-0035.

[38] Tu, Y., Wu, J., Xu, G., Yang, X., Cai, R., Gong, Q., Zhu, R., and Huang, W. "Perovskite Solar Cells for Space Applications: Progress and Challenges," *Advanced Materials* Vol. 33, No. 21, 2021, p. 2006545. doi: https://doi.org/10.1002/adma.202006545

[39] Johnson, L., Carr, J. A., Fabisinski, L., Russell, T., and Smith, L. "Lightweight Integrated Solar Array (LISA): Providing Higher Power to Small Spacecraft," *13th International Engergy Conversion Engineering Conference*. 2015, p. 3896.

[40] Lockett, T. R., Martinez, A., Boyd, D., SanSoucie, M., Farmer, B., Schneider, T., Laue, G., Fabisinski, L., Johnson, L., and Carr, J. A. "Advancements of the lightweight integrated solar array and transceiver (LISA-T) small spacecraft system," *2015 IEEE 42nd Photovoltaic Specialist Conference (PVSC)*. IEEE, New Orleans, LA, 2015, pp. 1-6.

[41] Carr, J. A., Boyd, D., Martinez, A., SanSoucie, M., Johnson, L., Laue, G., Farmer, B., Smith, J. C., Robertson, B., and Johnson, M. "The Lightweight Integrated Solar Array and Transceiver (LISA-T): second generation advancements and the future of SmallSat power generation," *Small Satellite Conference*. Logan, UT, 2016.

[42] Carr, J. A., Johnson, L., Boyd, D., Phillips, B., Finckenor, M., Farmer, B., and Smith, J. C. "LISA-T part three: The design and space environments testing of a thin-film power generation and communication array," *Acta Astronautica* Vol. 205, 2023, pp. 267-280. doi: https://doi.org/10.1016/j.actaastro.2023.02.001

[43] Dankanich, J., Burke, L., Carr, J. A., Landis, G., Peshek, T. J., Zoloty, Z. C., and O'Brien, R. C. "Transformational Propulsion for Fast In-Space Transits," *AIAA SCITECH 2024 Forum*. 2024, p. 1808.

[44] Díaz, F. C., Carr, J., Johnson, L., Johnson, W., Genta, G., and Maffione, P. F. "Solar electric propulsion for human mars missions," *Acta Astronautica* Vol. 160, 2019, pp. 183-194.

[45] Dudzinski, L. A., Hack, K. J., Gefert, L. P., Kerslake, T. W., and Hewston, A. "Design of a solar electric propulsion transfer vehicle for a non-nuclear human mars exploration architecture," *26th International Electric Propulsion Conference, paper IEPC-99-181, Kitakyushu, Japan*. 1999.

[46] Lopez Jimenez, F., Sharma, A., Folkers, M., and Murphey, T. W. "Design and Characterization of a Trussed Collapsible Tubular Mast," *AIAA SCITECH 2024 Forum*. 2024, p. 0411.

[47] Murphey, T. W., Turse, D., and Adams, L. "TRAC boom structural mechanics," *4th AIAA Spacecraft Structures Conference*. 2017, p. 0171.

[48] John A Carr, F. V. T., II, and Austin T Bumbalough. "Method for fabricating a photovoltaic device using computer-controlled system." Vol. 10930812, United States of America as represented by the Administrator of NASA (Washington, DC), U.S.A, 2021.

[49] Carr, J. A., Thompson, F., and Bumbalough, A. "Initial steps towards a robotic solution for the manufacturing and assembly of thin-film space solar arrays," *Flexible and Printed Electronics* Vol. 8, No. 2, 2023, p. 025020.

[50] McMillon-Brown, L., Luther, J. M., and Peshek, T. J. "What would it take to manufacture perovskite solar cells in space?." ACS Publications, 2022.

[51] Samantaray, N., Parida, B., Soga, T., Sharma, A., Kapoor, A., Najar, A., and Singh, A. "Recent development and directions in printed perovskite solar cells," *physica status solidi (a)* Vol. 219, No. 6, 2022, p. 2100629.

[52] Landis, G. A., and Perino, M. A. "Lunar production of solar cells," *Biennial SSI/Princeton Conference on Space Manufacturing*. 1989.

[53] Patane, S., Joyce, E. R., Snyder, M. P., and Shestople, P. "Archinaut: In-space manufacturing and assembly for next-generation space habitats," *AIAA SPACE and astronautics forum and exposition*. 2017, p. 5227.

[54] Murphy, D. M., Eskenazi, M. I., McEachen, M. E., and Spink, J. W. "UltraFlex and MegaFlex-Advancements in Highly Scalable Solar Power," *3rd AIAA Spacecraft Structures Conference*. 2016, p. 1947.

[55] Banik, J., and Hausgen, P. "Roll-Out Solar Arrays (ROSA): Next Generation Flexible Solar Array Technology," *AIAA SPACE and Astronautics Forum and Exposition*. 2017, p. 5307.

[56] Banik, J., Kiefer, S., LaPointe, M., and LaCorte, P. "On-orbit validation of the roll-out solar array," *2018 IEEE Aerospace Conference*. IEEE, 2018, pp. 1-9.

[57] Chamberlain, M. K., Kiefer, S. H., LaPointe, M., and LaCorte, P. "On-orbit flight testing of the Roll-Out Solar Array," *Acta Astronautica* Vol. 179, 2021, pp. 407-414. doi: https://doi.org/10.1016/j.actaastro.2020.10.024

[58] Surampudi, R., Blosiu, J., Stella, P., Elliott, J., Castillo, J., Yi, T., Lyons, J., Piszczor, M., McNatt, J., and Taylor, C. "Solar power technologies for future planetary science missions," *Jet Propulsion Lab, California Institute of Technology*, 2017.

[59] Simon, A., Nimmo, F., and Anderson, R. "'Journey to an Ice Giant System: Uranus Orbiter and Probe," *Planetary Mission Concept for the 2023-2032 Decadal Survey*, 2021.

[60] Kinnison, J., Vaughan, R., Hill, P., Raouafi, N., Guo, Y., and Pinkine, N. "Parker solar probe: A mission to touch the sun," *2020 ieee aerospace conference*. IEEE, 2020, pp. 1-14.

[61] Kirmani, A. R., Durant, B. K., Grandidier, J., Haegel, N. M., Kelzenberg, M. D., Lao, Y. M., McGehee, M. D., McMillon-Brown, L., Ostrowski, D. P., and Peshek, T. J. "Countdown to perovskite space launch: Guidelines to performing relevant radiation-hardness experiments," *Joule* Vol. 6, No. 5, 2022, pp. 1015-1031. doi: https://doi.org/10.1016/j.joule.2022.03.004

[62] Kirmani, A. R., Ostrowski, D. P., VanSant, K. T., Byers, T. A., Bramante, R. C., Heinselman, K. N., Tong, J., Stevens, B., Nemeth, W., and Zhu, K. "Metal oxide barrier layers for terrestrial and space perovskite photovoltaics," *Nature Energy*, 2023, pp. 1-12. doi: https://doi.org/10.1038/s41560-022-01189-1

[63] Bodeau, M. "Current and voltage thresholds for sustained arcs in power systems," *IEEE Transactions on Plasma Science* Vol. 40, No. 2, 2011, pp. 192-200. doi: https://doi.org/10.1109/TPS.2011.2176932

[64] Tyler, D., Diedrich, B., Gauvain, B., Ramazani, S., Heaton, A., and Orphee, J. "Attitude Control Approach for Solar Cruiser, a Large, Deep Space Solar Sail," *45th Annual AAS Guidance, Navigation and Control (GN&C) Conference*. 2023.

[65] Johnson, C., Heaton, A., Curran, F., and Rich, D. "The solar cruiser mission: demonstrating large solar sails for deep space missions," *Presentation at the 70th International Astronautical Congress, Washington DC, USA*. 2019.